

# Development of an Indium Bump Bond Process for Silicon Pixel Detectors at PSI

Ch. Broennimann<sup>a</sup> F. Glaus<sup>a</sup> J. Gobrecht<sup>a</sup> S. Heising<sup>a</sup> M. Horisberger<sup>a</sup> R. Horisberger<sup>a</sup>  
H. C. Kästli<sup>a</sup> J. Lehmann<sup>a</sup> T. Rohe<sup>a,1</sup> S. Streuli<sup>b</sup>

<sup>a</sup>Paul Scherrer Institut, 5232 Villigen PSI, Switzerland

<sup>b</sup>ETH Zürich, IPP, 5232 Villigen PSI, Switzerland

---

## Abstract

The hybrid pixel detectors used in the high energy physics experiments currently under construction use a vertical connection technique, the so-called bump bonding. As the pitch below 100  $\mu\text{m}$ , required in these applications, cannot be fulfilled with standard industrial processes (e.g. the IBM C4 process), an in-house bump bond process using reflowed indium bumps was developed at PSI as part of the R&D for the CMS-pixel detector.

The bump deposition on the sensor is performed in two subsequent lift-off steps. As the first photolithographic step a thin under bump metalization (UBM) is sputtered onto bump pads. It is wettable by indium and defines the diameter of the bump. The indium is evaporated via a second photolithographic step with larger openings and is reflowed afterwards. The height of the balls is defined by the volume of the indium. On the readout chip only one photolithographic step is carried out to deposit the UBM and a thin indium layer for better adhesion. After mating both parts a second reflow is performed for self alignment and obtaining high mechanical strength.

For the placement of the chips a manual and an automatic machine were constructed. The former is very flexible in handling different chip and module geometries but has a limited throughput while the latter features a much higher grade of automatization and is therefore much more suited for producing hundreds of modules with a well defined geometry.

The reliability of this process was proven by the successful construction of the PILATUS detector. The construction of PILATUS 6M (60 modules) and the CMS pixel barrel (roughly 800 modules) will start in 2005.

---

## 1. Introduction

The CMS experiment, currently under construction at the Large Hadron Collider (LHC) at CERN (Geneva, Switzerland), will contain a hybrid pixel detector for tracking and vertexing [1]. It requires bump bonding with a minimal pitch of 100  $\mu\text{m}$  which is below the industrial standard. In order to

achieve the highest flexibility during prototyping and a fast turn-over an in-house bump bond process was developed. It makes use of the infrastructure present at the Paul Scherrer Institut (PSI). The process was successfully applied to the PILATUS 1M detector [2], a single photon counting hybrid pixel detector with an area of  $24.3 \times 20 \text{ cm}^2$ .

In this process sketched in Fig. 1 the bumps are deposited onto the sensor part of the hybrid pixel module while only a thin ( $\approx 1 \mu\text{m}$ ) indium layer is

---

<sup>1</sup> Corresponding author; e-mail: Tilman.Rohe@psi.ch

deposited just to increase the adhesion. The bumps (deposited on the sensor) are reflowed to balls before the parts are joined. For self alignment and to provide good mechanical strength a second reflow is performed after the chip flip procedure.

## 2. Bump deposition on the sensor

The metal deposition on the sensor is done in two separate lift-off steps followed by a reflow.

### 2.1. Underbump metalization

The under bump metalization (UBM) consists of three metal layers which are added on top of the last metalization layer of the sensor (see Fig. 1 (a)-(g)). The first one is about 10 nm titanium that acts as a barrier and an adhesive layer. It is followed by roughly 50 nm nickel which is wettable with indium and a roughly 50 nm thick protective gold layer.

This sandwich is deposited in a so-called lift-off process. First (after a cleaning procedure) a two-layer photoresist is spun onto the wafer. The lower one is a  $1.2 - 1.5 \mu\text{m}$  thick lift-off resist (LOR) which is not light sensitive. The top layer is a negative resist with a thickness of about  $3.5 \mu\text{m}$ . *Negative* means that the resist gets developed in the non-exposed areas and a light-field mask is used on which the bumps appear as dark points. After exposure (Fig. 1 (b)) the non-exposed parts of the resist are developed. As the LOR is not light sensitive it is over-developed and an overhanging edge, a so called *undercut*, is created (Fig. 1 (c)).

The choice of the resist polarity is purely historical. In the first attempts “generic” masks were used and the alignment was done using the bumps themselves. This requires a mask which is essentially transparent. The disadvantage of negative resist is its sensitivity to stray light. If during exposure light is scattered at a rough metal surface into the shadowed region of the bumps, some resist might harden there. This leads to an undeveloped resist layer remaining on the bottom of the openings. The deposited metal layer is removed with the resist. As the sensor metalization is large

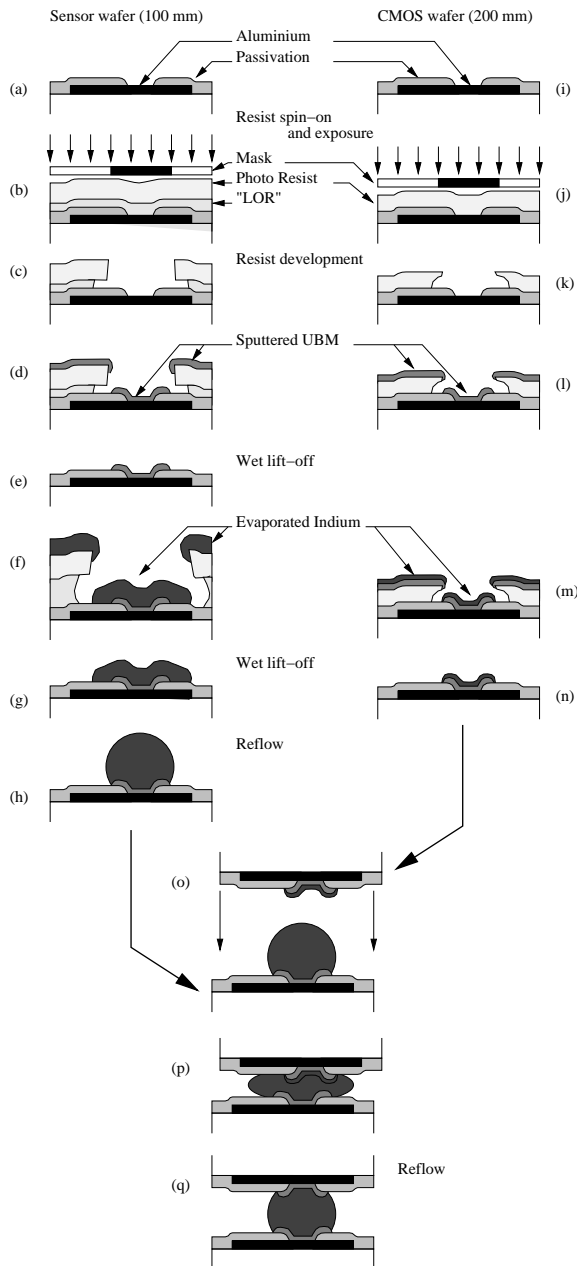


Fig. 1. Schematic flow diagram of the bump bonding process consisting of the bump deposition onto the sensor (a)-(h), metal deposition on the readout chip (i)-(n), and the flip chip procedure (o)-(q).

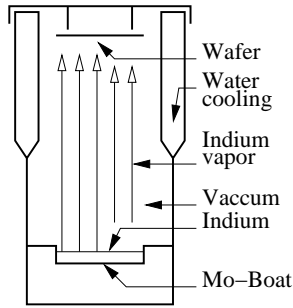


Fig. 2. Schematic cross section through the indium evaporation vessel. When the vacuum is established the indium in the molybdenum boat is heated. It evaporates and condenses on the wafer mounted on top.

around the bump pad and the surface is rather rough light scattering appears sometimes, but this effect is eliminated by the use of the LOR.

The deposition of the three metal layers (Fig. 1 (d)) is done in a multi-target magnetron sputtering machine. The thickness of the UBM is very small and cannot cover the overhanging edges of the resist.

When the photo resist is removed (lifted-off), the thin metal foil on top of it is also removed. The metal remains only in the area of the bump pad (Fig. 1 (e)). As the LOR is not soluble in acetone, this process has to be done with a special remover at an elevated temperature of about  $60^{\circ}\text{C}$ . The area of the deposited metals is very small causing this lift-off process to be slow. Process times of more than 12 hours are common.

## 2.2. Indium bump deposition

The indium bumps are deposited using a similar lift-off process. The only difference is the thickness of the resist and the increased size of the openings. To safely exceed the layer thickness of the evaporated indium of  $2 - 3\ \mu\text{m}$ , the resist is spun on with a total thickness of about  $8\ \mu\text{m}$  ( $3.5\ \mu\text{m}$  LOR plus  $4.5\ \mu\text{m}$  photoresist).

The indium is deposited in a 50 cm high cylindrical vessel (see Fig. 2) with a diameter of about 30 cm that can be evacuated down to a few  $10^{-5}$  mbar. When this level is reached the indium in a molybdenum boat at the bottom is heated. It evaporates and condenses on the wafer mounted at

the removable top cover. The side wall of the vessel is water-cooled which considerably reduces the thermal budget on the photoresist. By this measure blaining of the resist is prevented. Further the resist hardens if it is exposed to too much heat and its removal becomes difficult.

The removal of the photoresist is done similarly to the UBM process. After the lift-off the indium forms a rather flat octagon as shown in Fig. 3 (a). As the bumps are relatively insensitive to mechanical damage in this state and the wafers can be handled without special care, it is the right moment to dice the wafers and again test the individual sensors on a probe station.

## 2.3. Reflow

In order to form balls from the indium the devices have to be heated. When the indium is molten, the balls are created by the surface tension. The size of the ball is defined by the diameter of the wettable UBM pad and the volume of the evaporated indium. The result of the reflow process is shown in Fig. 3. The distance between the bumps is  $100\ \mu\text{m}$ . The width of the deposited indium octagon is in this case  $50\ \mu\text{m}$  and its thickness is about  $2\ \mu\text{m}$ . This leads to a volume of about  $4000\ \mu\text{m}^3$  per bump or a bump diameter of about  $20\ \mu\text{m}$ .

The reflow is performed in a microprocessor controlled oven, regulating temperature profile, flux gas pressure, etc. which was designed and built at PSI.

## 3. Metal deposition on the readout chip

For the readout chips the same lift-off mask is used for the UBM and the indium as indicated in Fig. 1 (i)-(n). This is possible because the amount of indium deposited on the chips is much smaller and no bump balls will be formed here. As the metal surface of the CMOS wafers is usually very plain and stray light is not an issue, the use of lift-off resist (LOR) is not necessary. Only a layer of about  $3.5\ \mu\text{m}$  negative resist is spun onto the 200-mm-wafers. The undercut of the edges is created

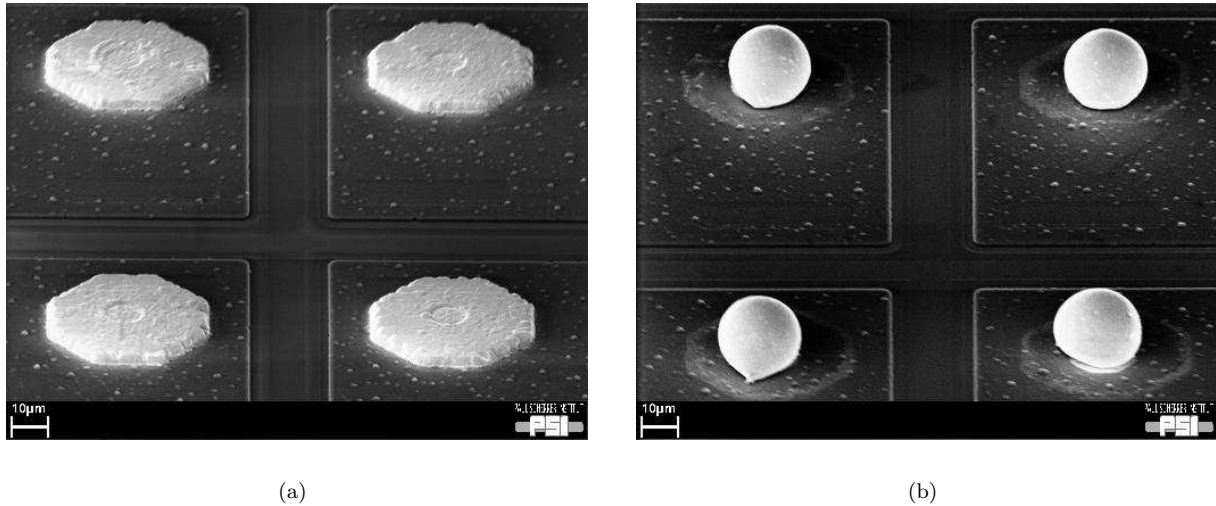


Fig. 3. A scanning electron micrograph of indium bumps before (a) and after (b) reflow. The distance between the bumps is 100 μm, the deposited indium is 50 μm wide, the reflowed bumps have a diameter of about 20 μm.

by a suitable choice of exposure and development times.

The UBM is then sputtered onto the wafer directly followed by the evaporation of a thin 1–2 μm indium layer. Due to the use of “normal” photoresist, the lift-off can be done at room temperature using acetone.

After the lift-off process the wafers are thinned and diced. The task of the thin indium layer is to improve adhesion after the chip flipping. The chips are however not reflowed before the flip chip procedure.

#### 4. Chip placement

The readout chips and the sensors are joined to form a *bare module*. As in most cases several readout chips (16 for CMS and PILATUS modules) are placed onto one sensor, the latter is mounted on a table and the chips are placed successively. This is done either in a manual or automatic chip placement machine. While the former is very flexible and used for prototype and single chip assemblies, the latter is automated to a high degree and allows the throughput necessary for the construction of larger pixel detectors. After the placement of the

chips, the modules are reflowed to establish the mechanical connection. Further the surface tension of the molten indium provides self-alignment (see Fig. 1(o)-(q)).

After the reflow, the module is robust enough for further handling and will be tested before being fed it into the module production line.

##### 4.1. Manual chip placement

The manual chip placement machine was designed for the fast and flexible production of a small quantity of modules in the prototyping stage of the CMS pixel detector. Its working principle is schematically shown in Fig. 4. The sensor is mounted onto a movable stage while the readout chip is held with its face down on a vacuum chuck. Both parts can simultaneously be observed through a prism. When both parts are aligned with respect to each other, the prism is removed and the chuck with the readout chip is pressed onto the sensor. A force up to about 50 N is applied.

The machine is designed and constructed to flexibly handle different module sizes and geometries which is very important in the R&D phase of a project. However, the manual alignment procedure is somewhat tedious and results in 3–4 h needed for

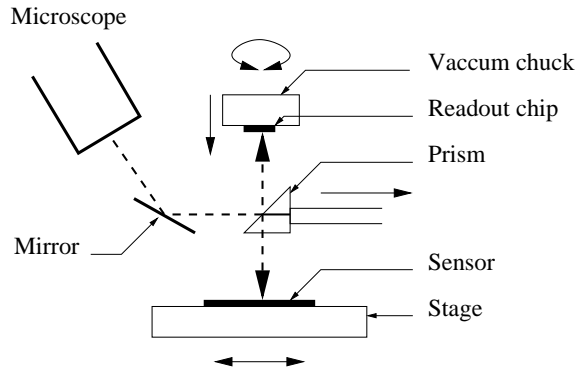


Fig. 4. Schematic diagram of the working principle of the manual chip placement machine. Both parts are aligned in respect to each other using a prism placed in between them. After alignment the prism is removed and the chip is pressed onto the sensor.

the placement of 16 chips on a sensor. The throughput of the machine is limited to a few modules per week which is not sufficient for building detectors with hundreds of modules.

#### 4.2. Automatic chip placement

In order to overcome the limitations of the manual chip placement machine, a fully automated one, shown in Fig. 5, was designed and built. It consists of a table which can automatically move with a precision of one micrometer in the horizontal plane. The vertical movements and possible rotations are performed with the pick-and-place tool which is fixed to the very massive bridge.

After equipping the table with the sensor and the readout chips, the position of the sensor is precisely measured with a microscope mounted next to the pick-and-place tool. This is done automatically using alignment marks on the sensor and a pattern recognition algorithm.

Then a first read-out chip placed face down on a gel-pack is picked by the pick-and-place-tool and held by vacuum. Its position is also precisely measured with the microscope looking up which is integrated into the moving table. The chip undergoes an electrical functionality test using the probe card mounted on that table. Only working chips are placed on the sensor. Placing can be done as the sensor and chip position within the machine frame

are known from the position measurements. It is pressed down with a force of 30 N (about 8-10 mN per bump) and held for 1 min. This procedure is repeated for all 16 readout chips.

In case one of the chips does not pass the electrical test, it is put back onto the gel-pack and a reserve chip from an additional gel-pack (not visible in Fig. 5) is used instead. This should rarely happen as all chips were tested on-wafer and only good dies are picked from the dicing tape. However, during the dicing and picking procedure and the subsequent handling a small fraction of the chips might be damaged.

The placement of 16 chips on a sensor takes about 50 min including the chip test plus about 15 min for loading the machine and preparing the components. During the chip placement no human intervention is necessary. This allows a throughput of several modules per day, sufficient for the construction of a vertex detector with some hundreds of modules.

#### 4.3. Reflow

After the chip placement is finished the assembly undergoes a second reflow similar to the one described in Sect. 2.3. As the module is very fragile before this step, the transfer from the chip placement machine to the reflow oven has to be done with special care. After melting a stable mechanical connection is established. Further the surface tension of the indium in addition provides self-alignment.

#### 4.4. Tests

The reflowed module, called the *bare module*, is robust enough for handling, and tests can be performed.

##### 4.4.1. Pull test

A correctly joined assembly is resistant to about 2 mN pulling force per bump which adds up to about 8 N for a CMS-readout chip with 4160 bump bond connections. To test the quality of the bumps, every chip is pulled with a force of about 1.8 N applied through a vacuum cup. If this test fails,

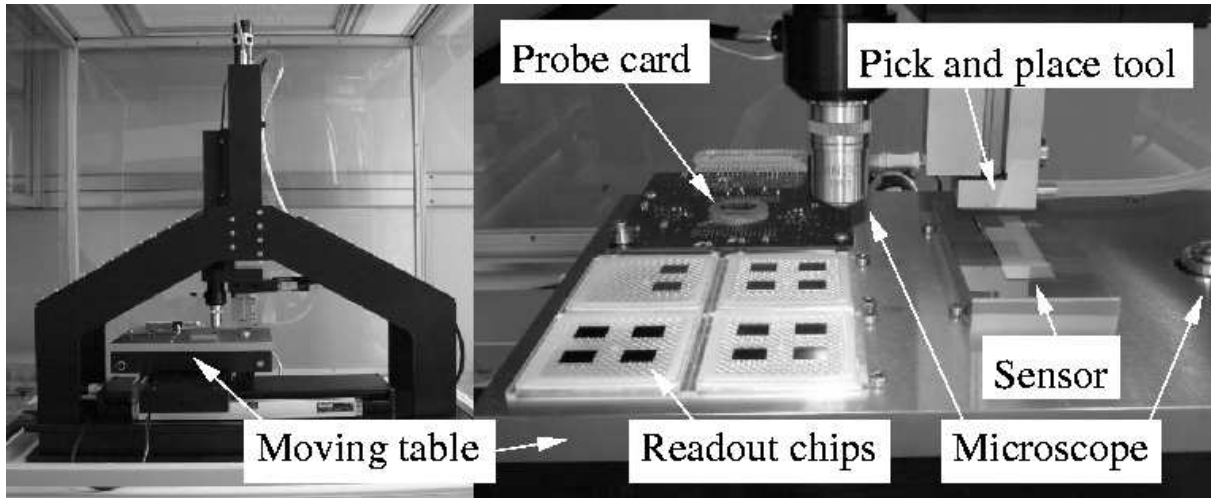


Fig. 5. Automatic chip placer.

which happens very rarely, it is an indication for a serious mistake either during chip placement or reflow. In this case the module is excluded from all further production steps and the reason for the failure has to be investigated.

#### 4.4.2. Geometrical verification

A very efficient way of testing the correctness of the chip placement is to measure the distance between readout chips. Due to the self alignment during the reflow, the distance between the readout chips in a correctly bump bonded module differs by less than five micrometres from its nominal value.

The measurement of the distance can easily be performed using the automatic chip placement machine. The bare module is positioned with the chips down on the moving table and the distance between alignment marks on the chip parts that extend over the edge of the sensor can be measured automatically.

If a chip is found to be misplaced the module is excluded from all further processing. This would indicate a serious error during chip placement or handling.

#### 4.4.3. Tests of the readout chips

While failure modes described in Sect. 4.4.1 and 4.4.2 are expected to occur only in the prototyping stage, when the procedures are not yet well

established, the experience of other pixel projects [3,4,5] shows that the failure of readout chips after bump bonding cannot completely be avoided. The damage is often caused by silicon pieces which fall off the chip edges during or after dicing. If the size of such a piece exceeds the bump height, it is pressed into the surfaces of the sensor or/and the readout chip which in most cases causes serious damages such as power shorts in the readout chip. In order to detect such failures each chip of a bare module is tested with a probe card.

#### 4.5. Rework

If a faulty chip is detected on a bare module it is not further assembled. However, at this stage of the module assembly it is still possible to replace chips.

To remove a readout chip the bare module is placed on a heatable chuck and held by vacuum as shown in Fig. 6. The removal tool is then lowered onto the faulty readout chip and is also heated. When a sufficient temperature is reached the chip is grasped by vacuum and the tool is lifted. The heating temperatures and the lifting speed have to be adjusted in a way that the indium balls stick to the sensor and not to the readout chip.

After this procedure a new readout chip can be placed in the vacant position and the reflow has to

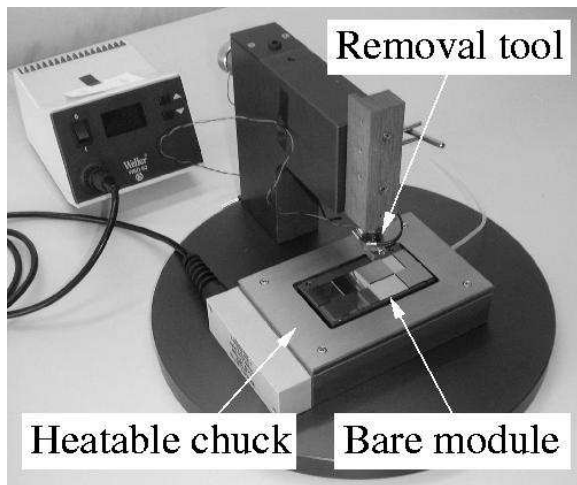


Fig. 6. Tool for removing a readout chip from a bare module

be repeated. The bump yield of replaced chips will not reach the level of the initial ones and therefore all measures to minimize the fraction of bare modules to be reworked are taken. A careful inspection and cleaning of the readout chips as single dies is essential. The introduction of a dry cleaning step using a very soft sponge just before the flip chip procedure has reduced the number of chip failures drastically.

The completely tested bare module is then glued onto a base plate. At this point a repair is not possible anymore. A complete description of the module assembly is given in [6].

## 5. Bump yield

The bump yield of a module can be measured either directly with particles and X-rays or indirectly using the influence of the bump bond connection on the analogue behavior of the readout chip as discussed in Ref. [7].

The bump yield determination of a PILATUS module with X-rays is illustrated in Fig. 7. As a first step the electronics channels not responding to calibration pulses are detected. The black pixels following a circular shape in the upper middle of Fig. 7 (a) probably suffer from a localized high sensor current leading to a saturation of the pixels' preamplifiers. These pixels are excluded from

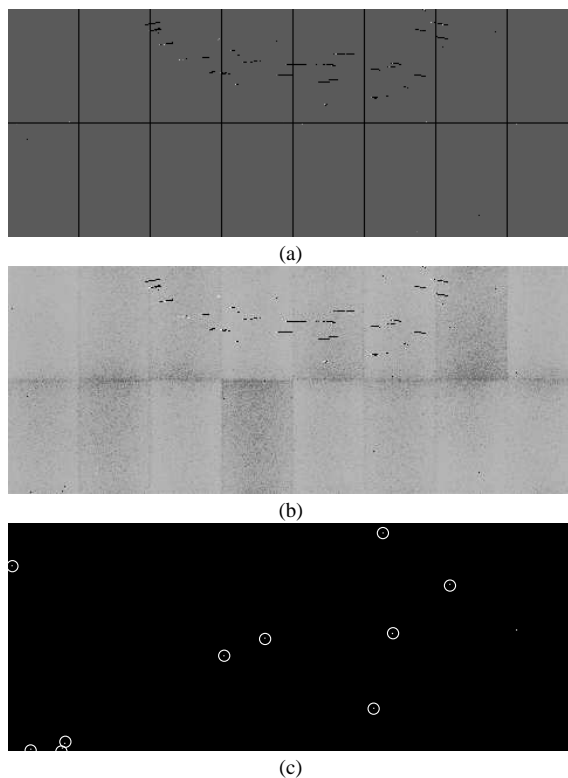


Fig. 7. Determination of the bump yield using illumination with X-rays. (a) Determination of broken channels in the readout chips, (b) illumination with X-rays, (c) missing bump bonds are marked with circles

further analysis. As the second step the response of the module to X-rays is measured as shown in Fig. 7 (b). The number of dead channels is determined by looking for pixels which do respond to calibration pulses but not to X-rays. In this case ten pixels (see Fig. 7 (c)) were found representing a fraction of less than 0.05%.

The experience gained with the production of a few tens of modules and some hundreds of readout chips shows that, if no problems in the photolithographic steps occur, the bump yield is either above 99.9% or the bump bonding fails completely (bump yield < 90%). The occurrence of such fails is rare and indicates a fundamental problem in the assembly procedure of this particular module.

## 6. Conclusions

A bump bonding process was developed at PSI in the framework of the R&D for the CMS pixel detector. It features an underbump metalization composed of titanium, nickel and gold on both sensor and readout chip. The indium bumps of about 20  $\mu\text{m}$  height are deposited onto the sensor and reflowed, while on the readout chip only a thin indium layer is evaporated. After both parts are joined another reflow is performed to establish the thermo-mechanical connection and to perform self alignment.

The bump yield of successfully built modules exceeds 99.9%. The fraction of such modules is not yet known, but the present experience is very encouraging and there is hope to achieve a sufficient yield without reworking.

The process was used to build the PILATUS 1M pixel detector with 18 modules [2]. The commissioning of a fully automatic chip placer increases the throughput considerably and the construction of large systems requiring hundreds of modules, like the CMS pixel detector, becomes feasible and will start in early 2006.

## 7. Acknowledgments

Thanks are due to Stefan Ritter for the micrographs of the bumps (Fig. 3) and Beat Henrich for providing the bump yield measurement (Fig. 7).

### References

- [1] The CMS Collaboration, CMS Tracker, Technical Design Report LHCC 98-6, CERN, Geneva, Switzerland (1998).
- [2] G. Hülsen, C. Broennimann, E. F. Eikenberry, Distortion calibration of the PILATUS 1M detector, NIM A 248 (2005) 540–554.
- [3] P. Riedler, et al., Overview and status of the ALICE silicon pixel detector, these proceedings.
- [4] G. Alimonti, et al., Analysis of the production of ATLAS pixel modules with indium, these proceedings.

- [5] T. Fritzsich, Experiences in fabrication of multichip-modules for the atlas pixel detector, these proceedings.
- [6] S. König, et al., Assembly of the CMS pixel barrel modules, these proceedings.
- [7] A. Starodumov, et al., Qualification procedures of the CMS pixel barrel modules, these proceedings.